NASA Technical Memorandum 4246

A Methodology for Designing Aircraft to Low Sonic Boom Constraints

Robert J. Mack and Kathy E. Needleman

FEBRUARY 1991

NASA

NASA Technical Memorandum 4246

A Methodology for Designing Aircraft to Low Sonic Boom Constraints

Robert J. Mack
Langley Research Center
Hampton, Virginia

Kathy E. Needleman
Lockheed Engineering & Sciences Company
Hampton, Virginia

National Aeronautics and
Space Administration
Office of Management
Scientific and Technical
Information Division

1991

Abstract

A method for designing conceptual supersonic cruise aircraft to meet low sonic boom requirements has been outlined and described. The aircraft design is guided through a systematic evolution from an initial three-view drawing to a final numerical model description while the designer using the method controls the integration of low sonic boom, high supersonic aerodynamic efficiency, adequate low-speed handling, and reasonable structure and materials technologies. Some experience in preliminary aircraft design and in the use of various analytical and numerical codes is required for integrating the volume and lift requirements throughout the design process.

Introduction

Methods for minimizing sonic boom ground overpressures have been devised and published since Whitham introduced his supersonic wave propagation theory (ref. 1) in 1952, and Walkden (ref. 2) showed that Whitham's theory could be applied to analyzing lifting wing-body shock patterns. Using Whitham-Walkden theory, Jones (ref. 3) predicted that severe nose blunting on a slender body of revolution or on an equivalent-area body representing volume and lift would measurably decrease far-field ground overpressures. However, this reduction in far-field overpressure strength was accompanied by an increase in aerodynamic drag. The drag penalty dampened hope for effective sonic boom minimization through aircraft design until McLean (ref. 4) showed that a far-field overpressure signature might not fully develop if the aircraft were long and slender without excessive weight increase. Carlson, McLean, and Shrout (ref. 5) showed that when the aircraft volume and lift were shaped and integrated such that their summed equivalent areas followed a Mach-sliced $x^{3/2}$ area growth curve, ground overpressures less than the far-field minimums could be obtained without appreciable drag penalty. In 1972, Seebass and George (ref. 6) formalized near-field minimization procedures that included a small degree of nose blunting. These formulations reduced near-field overpressures below levels estimated by Carlson, McLean, and Shrout, although some attendant drag penalties were still possible. A numerical technique for obtaining near-field overpressure signatures was developed by Middleton and Carlson (ref. 7) with input from both the analytically smooth shapes treated by McLean and Seebass as well as the arbitrary volume and lift distributions derived from actual aircraft.

These theoretical reduced-overpressure benefits prompted a study (ref. 8) of the potential results from applying minimization theory to conceptual aircraft design and performance. Minimization theory and aerodynamic efficiency considerations were used to guide the conceptual aircraft design, and Whitham theory was used to predict the level of reduced ground overpressures possible with each configuration. The results of this design study pointed to weight reduction, center of gravity control, and aerodynamic efficiency as key factors to be monitored during the design process. A follow-up study (ref. 9) corroborated these conclusions while showing that a more rigorous application of minimization theory produced conceptual aircraft designs meeting most of the mission requirements, especially those of low sonic boom and high aerodynamic efficiency.

Minimization theory reached its present stage of development when Darden (ref. 10) modified the Seebass and George minimization theory by making the "nose bluntness" a variable parameter. This subtle change permitted low-boom characteristics to be traded with reduced wave drag. A theoretical and experimental study (ref. 11) tested this modified theory with a series of wing-body wind-tunnel models. The test results validated the modified minimization theory at a Mach number of 1.5 and suggested that it could also be applicable at a Mach number as high as 2.7.

These minimization methods provided low-boom equivalent-area constraint curves for the sum of the volume and lift contributions, but gave no information about aircraft configuration geometry or component shapes that could satisfy both low-boom and high aerodynamic efficiency requirements. For instance, the three low-boom wind-tunnel models used in reference 11 and two of the conceptual aircraft studied in references 8 and 9 had a number of sonic boom reducing features, but there were other aircraft designs with similar features that could have met the same low-boom constraints. Moreover, the scope of these studies precluded a detailed discussion of how various system requirements as well as low-boom constraints were integrated into the design of the configuration.

In this report, a flexible but systematic method for designing conceptual aircraft to meet low sonic boom constraints is outlined and explained. The method is based on the premise that the wing planform shape is the basic starting point for a high-speed civil aircraft design. Fuselage, engines, and control surfaces are incorporated, sized, and integrated as the configuration evolves toward a candidate aircraft capable of meeting the mission requirements. To achieve this goal, the method guides the aircraft design from an initial three-view drawing to a candidate configuration that has low-boom characteristics and is ready for a full mission and performance

evaluation. The analytic methods, computer-implemented design codes, and empirical methods used to design the aircraft and analyze its sonic boom characteristics are listed and referenced. An example is presented to demonstrate the use of the analysis codes and design tools within the framework of the design method.

Symbols

A_E	equivalent cross-sectional area, ft^2
C_L	lift coefficient
$C_{m,o}$	pitching-moment coefficient at zero lift
$F(\tau)$	Whitham F-function with variable τ
h	cruise altitude, ft
ℓ	length, ft
ℓ_E	effective length, $\ell + \beta z(\ell)$, ft
M	Mach number
Δp	overpressure; local pressure minus free-stream pressure, psf
W	beginning cruise weight, lb
x	longitudinal distance or length, ft
x_E	effective length in flight direction, ft
y	spanwise distance, ft
y_f	"nose bluntness" parameter, ft (see fig. 2)
z	displacement from x-y plane, ft
α	angle of attack, deg
β	Mach number parameter, $\sqrt{M^2 - 1.0}$
ζ	dihedral height, ft
λ	length where tail constraints begin (see fig. 2), ft
Λ_{LE}	leading-edge sweep angle, deg
μ	Mach angle, $\sin^{-1}(1.0/\mathrm{M})$, deg
τ	Whitham F-function variable

Subscripts:

N	nose shock
T	tail shock

Analytic Tools

A large number of existing computer-implemented design and analysis codes can be used to generate a low-boom-constrained supersonic cruise configuration. Those used in the design method described in this report were

1. Boom minimization code (ref. 10)
2. Wave drag code (ref. 12)
3. Wing performance analysis code (ref. 13)
4. Nacelle-wing interference lift code (ref. 14)
5. Supersonic wing optimization code (ref. 15)
6. Sonic boom propagation code (ref. 16)
7. F-function and shock system calculation code (ref. 7)
8. Fuselage normal area calculation code (ref. 17)

Sources for the derivations and the descriptions of these design and analysis codes are in the references and will not be repeated in the text. Some of them may be obtained from

Computer Software Management and Information Center (COSMIC)
112 Barrow Hall
University of Georgia
Athens, Georgia 30602
(404) 542-3265

These references and their designation numbers are as follows:

Reference 10: LAR-11979
Reference 12: LAR-13223
Reference 13: LAR-12788
Reference 16: LAR-10480
References 12, 14, 15: LAR-12857

Design Method

An illustrative schematic diagram of the design method for designing low sonic boom conceptual aircraft is presented in figure 1(a). The method consists of a two-cycle aircraft design and modification part (left-hand side) and a minimization constraint calculation part (right-hand side) as seen in figures 1(a) to 1(c). Both the aircraft geometry and the low sonic boom minimization constraints are derived from parameters given in the mission requirements. As the aircraft geometry evolves in each of the two design cycles, its net equivalent areas are computed and compared with ideal equivalent areas calculated from low-boom constraints. In the following sections, each part of this method will be explained, and their interactions to generate the low-boom aircraft planform and geometry will be demonstrated.

Low Sonic Boom Constraints

Both design cycles require a comparison of aircraft equivalent areas with the theoretical low-boom equivalent areas calculated by the minimization code from the following parameters:

1. Cruise Mach number
2. Cruise altitude, ft
3. Aircraft effective length, ft
4. Aircraft beginning-cruise weight, lb
5. "Nose bluntness" parameter length, ft
6. Ratio of nose shock Δp to tail shock Δp, usually 1.0

The output from the boom minimization code is one of two possible Whitham F-functions, which mathematically describe pressure disturbance shapes and strengths along the aircraft's equivalent-area body, a constrained equivalent-area curve, and a ground-level signature derived from the F-function and propagation through a standard stratified atmosphere from cruise altitude to the ground. Four of the input parameters—Mach number, altitude, nose bluntness, and $\Delta p(\text{nose})/\Delta p(\text{tail})$ ratio—influence the configuration size, weight, and shape, but, in order to obtain an initial pressure signature, these input values will be considered as constant in the initial iteration.

Values of beginning cruise weight and effective length will probably change as the design of the aircraft configuration evolves. These changed weight and length values are used as new input values to the minimization code, obtaining another equivalent-area constraint curve when the new overpressure strength equals or is less than the required overpressure limit. This application flexibility reduces the time required to bring the minimization code constraint areas and the configuration's equivalent areas to acceptable agreement.

Figure 2 shows the two minimized low-boom Whitham F-functions and ground overpressure signatures theoretically possible. At present it is not known which of the two pressure signatures is more annoying to human listeners if both signatures have the same nose shock strength. Experience has shown that for a given nose shock strength, the aircraft designed to generate the F-function and pressure signature shown in figure 2(b) will be shorter and potentially lighter than an aircraft designed to generate those in figure 2(a). However, an aircraft designed to generate the figure 2(a) F-function will generate a ground overpressure signature that is less perturbed by small variations in the propagation characteristics of the atmosphere from cruise altitude to the ground. This is because the nose-shock condition can be satisfied along a constant value of $F(\tau)$ for $y_f < y < \lambda$ rather than at the point $y = y_f$.

Aircraft Design

Overall mission requirements strongly influence the choices of wing planform, fuselage length and maximum diameter, number and size of engines, and the resulting aircraft effective length. These parameters, in turn, are the factors used to estimate the gross takeoff weight and the beginning cruise weight needed to start the design process. Experience and personal design philosophies often guide the choices of planform shape and the estimates of weight. As a help in making some of these initial estimates, previous supersonic cruise aircraft studies are some of the best sources of information.

Cycle 1. The initial wing planform is given a flat camber surface (as indicated in figs. 1(a) and (b)). Changes can then be readily made without the repetitive, time-consuming reworking of a camber surface tailored to a specific planform. Constant maximum thickness airfoils, a simple fuselage, a fin or fins, and a set of engine nacelles are added to complete an initial configuration and three-view. If additional effective length will help to meet low-boom constraints, modest wing dihedral could also be included. Figure 3 shows the effect of wing dihedral on the effective lifting length and how it can be used to offset the reduction in effective length due to angle of attack. The effective length ℓ_E corresponds to the aircraft length ℓ while $\ell_{E,1}$ is the wing effective length without dihedral. With dihedral height ζ, the wing effective length increases from $\ell_{E,1}$ to $\ell_{E,2}$. However, dihedral must be added cautiously since it can adversely alter the yaw-roll stability characteristics of the aircraft.

A numerical model, derived from this initial three-view, provided input to the wing analysis code (ref. 13), the wave drag code (ref. 12), and the interference lift code (ref. 14). The output from these codes provides initial estimates of zero-lift wave drag, the lift curve slope, and equivalent areas that are summed and compared with the ideal equivalent areas obtained from the minimization code (ref. 10) (comparison box in fig. 1(b)). Reasonable agreement is reached when the aircraft equivalent areas are close to, but less than, the ideal equivalent areas with some equivalent area increments reserved for the introduction of camber and twist.

This reasonable agreement decision is a judgment skill achieved by experience and cannot be described quantitatively. However, small adjustments to the equivalent areas are still possible with wing thickness and, as will be described, with fuselage area.

Cycle 2. Having fixed the planform shape on an initial configuration, camber and twist are introduced and Cycle 2, figure 1(c), is entered. The initial three-view permitted center of gravity and aerodynamic center locations to be estimated. Then,

the calculated wing camber ordinates are scaled to provide from one-quarter to one-half of the required cruise C_L and most of the $C_{m,o}$ required for self trimming. Residual $C_{m,o}$ obtained from the estimated interference moments and the residual C_L necessary to maintain cruise altitude are obtained from flat-plate lift (angle of attack) and interference lift data. The most convenient fuselage position is the coincidence of the wing root camber line and the fuselage centerline. Changes from this alignment will introduce fuselage-on-wing and wing-on-fuselage interference increments but may help in meeting low-boom constraints, decreasing floor angle requirements, or improving structural integration. Following the integration and blending of the wing and the fuselage, the nacelles and the fin(s) are positioned, usually in their locations before the introduction of wing camber and twist. When these steps are completed, the wing lift and nacelle-wing interference lift distributions are computed.

Volume and lift equivalent areas from the aircraft design are obtained from the wave drag, wing analysis, and interference lift code predictions. This aircraft equivalent area is compared with the low-boom constraint curve and judged for closeness of agreement. From this stage onward, wing and/or fuselage thickness can be added to bring the aircraft equivalent areas into coincidence with the boom-constrained equivalent areas. Should this result in an aircraft with high zero-lift drag, unacceptable trim drag penalties, unacceptable center of gravity travel, etc., a new planform and a new camber surface will probably be needed. This will mean returning to the uncambered wing design cycle, but eventually a conceptual/candidate aircraft design will be found that satisfies low-boom criteria.

Example of Configuration Design

The design process will be explained further by going through the design of a conceptual Mach 2 supersonic cruise aircraft. The procedures outlined will demonstrate the application of sonic boom minimization to achieve low-boom characteristics. Initial design and optimization parameters of

$M = 2.0$
$h = 55\,000$ ft
$\ell_E = 250$ ft
$W = 550\,000$ lb
$y_f = 30$ ft

obtained from the mission requirements were used to obtain an equivalent-area distribution, a Whitham F-function, and a minimum overpressure ("flat top" or plateau) signature (fig. 4) that had nose and tail shocks of

$$\Delta p_N = \Delta p_T \cong 1.046 \text{ lb/ft}^2$$

Ground overpressure strength is dependent on these five parameters. If the resultant overpressure is unsatisfactory, then variations in the input values (especially y_f, which usually is initialized at $\ell_E/10.0$) may provide acceptable overpressure values without seriously compromising the mission or design requirements. Rather than run such a parametric study, the $\Delta p_N = \Delta p_T \cong 1.046$ lb/ft^2 value is considered as an acceptable upper limit to start the design. During the design process, additional considerations will be mentioned and applied to make the resulting aircraft as aerodynamically efficient as possible.

All aircraft configurations have component shapes and arrangements that reflect different design philosophies: wing(s) with or without dihedral or camber and twist, circular or integral fuselage(s), canard/horizontal tail, vertical tail(s), and engine nacelle(s) that must be integrated into a final, practical shape. A wing/body/four-engine, four-nacelle/fin configuration was chosen to meet the design requirements with a minimum of component and integration complexity.

Wing

The initial wing planform chosen, figure 5, incorporated many of these low-boom features:

1. Long lifting length, about 300 ft
2. Slender airfoil shape and thickness ratio, about 2.5 percent
3. High leading-edge sweep over a large fraction of the semispan with $\beta \cot \Lambda_{LE} < 1.0$
4. Rounded "platypus nose" wing apex
5. Wing dihedral

The arrow wing part of the planform was initially given a 160-ft span with a supersonic leading edge along the outer wing panel to help low-speed performance while keeping a long lifting length. A strake with a highly swept leading edge, $\Lambda_{LE} = 82.9°$, and a rounded "platypus nose" vertex were added to extend the lifting length and to quickly initiate the lift equivalent area growth. At the initial angle of attack required for level cruise flight, about 9° of dihedral was used to maintain the effective length of about 300 ft. When camber and twist were introduced, some dihedral was also included to keep the lifting length as close as possible to the initial value.

Fuselage

The initial fuselage length, about 300 ft, and diameter, about 12 ft, were determined by the number

of passengers (250+) and crew (10); the proposed seating (5 to 6 abreast); and by provision of room for the cockpit, lavatories, exits, galleys, baggage, and reserve fuel. It had an ogive-cylinder-ogive shape and an uncambered mean line. With the introduction of wing camber and twist, the fuselage camber line was modified to blend smoothly with the root chord section. As the final equivalent-area adjustment was done, the fuselage shape was altered to make the sum of the configuration's volume and lift equivalent areas agree with those that minimization theory predicted for a specified low-boom signature.

Engine Nacelles

Studies of other conceptual supersonic cruise aircraft designed for similar payloads and ranges indicated that takeoff requirements usually sized the engines while supersonic cruise requirements usually sized and shaped the inlet. Each inlet/engine/nozzle nacelle used on the conceptual Mach 2 aircraft was sized from a generic engine nacelle to have a length of 44 ft and a maximum diameter of 5.5 ft. They were grouped in pairs and located near the inboard trailing edge of the wing so that their volume and interference lift equivalent areas were kept to a minimum. Idealized engine operating conditions at cruise were assumed so that the exhaust plumes could be modeled as constant-area cylinders.

Vertical Tail(s)

Takeoff with one-engine-out conditions were used to compute the area of the vertical tail(s) once the position(s) on the aircraft had been decided. Since they can be well aft on the configuration, their volume can influence the effective length but will seldom provide sizable contributions to the net equivalent areas. The single vertical tail on the conceptual Mach 2 configuration required about 675 ft^2 of area and was located on the aft upper fuselage with its leading edge starting about 230 ft from the nose.

Initial Three-View

The initial conceptual design components were integrated as shown in figure 6. Although the aircraft plan-view length was 300 ft, angle of attack gave it an effective length of about 250 ft. A numerical model of this configuration was used as input data to the wave drag, wing analysis, and interference lift codes so that equivalent-area distributions from volume and lift could be calculated. In figure 7, a comparison of the low-boom-constrained and initial conceptual aircraft equivalent areas are shown. The two curves are not close, showing that sizable modifications to the initial design are needed to obtain an acceptable configuration.

Design Evolution

A series of judicious changes made in the planform produced the configuration shown in figure 8 and the equivalent-area distribution shown in figure 9. The wing apex "platypus nose" was reduced and the forward wing panels were given a higher sweep angle to allow more room for fuselage passenger space and more effective area for the effects of camber and twist. Leading-edge blending was used to give more smoothness to the curve of equivalent area due to lift from forward wing strake to outboard wing tip. Extra fin area was added for control effectiveness when the fin area centroid was found to be closer than expected to the calculated aerodynamic center and probably to the yet-to-be-determined center of mass as well. A change of inlet from a two-dimensional to an axisymmetric design shortened the nacelle to a length of 33.5 ft. This decreased the interference effects of nacelle on wing and potentially reduced nacelle, nacelle strut, and wing spar weight. A comparison of equivalent areas, figure 9, showed that more aircraft equivalent area had been removed than required and indicated that the effective length could be increased, which would decrease the theoretical low-boom overpressure level.

Taking advantage of this design opportunity, new low-boom equivalent areas were calculated with the effective length increased to 270 ft. Shortening the nose bluntness length to 20 ft in order to obtain a better equivalent area agreement near the nose, a new low-boom ground overpressure of 0.955 lb/ft^2 was possible. The increase in effective length also permitted the dihedral to be decreased from 9° to a more reasonable 4.6° and decreased the potential for yaw-roll tendencies, which are often present in aircraft with wings whose leading edges are highly swept. This more modest dihedral was incorporated into the wing camber and twist.

The fuselage was also affected by the wing camber since its centerline was coincident with the wing root chord camber line. With a cruise angle of attack of 0.60° the floor angle through the main passenger sections was about 4°. If a 4° floor angle is considered excessive, the fuselage centerline could be shifted vertically to a more acceptable slope. Then, by carefully matching the fuselage area growth above the wing to the fuselage area growth below the wing, keeping the total fuselage area growth within low sonic boom constraints, all three requirements of floor angle, aircraft drag, and low boom could be met.

These design modifications changed the Mach 2 conceptual aircraft design from that shown in figure 8 to the one shown in figure 10. The results of the new low-boom constraint area curve calculation and the new equivalent areas from the evolving design are shown in figure 11. A very small gap now separated the two equivalent-area curves—a gap that could be closed by suitable modifications to the area distribution of the fuselage. First, the required fuselage equivalent areas were found by subtracting the lift equivalent areas and the aircraft wing, fin, and nacelle volume equivalent areas from the low-boom-constrained equivalent areas. Then, using the fuselage camber line ordinates and the computer code of reference 15, a distribution of fuselage normal areas was found that would produce the required equivalent areas. This process of determining a distribution of normal areas to produce a desired distribution of equivalent areas required several iterations, with the wave drag code being used to check the progress of each step. In figure 12, both the desired fuselage equivalent-area distribution and the computed fuselage equivalent-area distribution are shown and compared. Since a reasonably close agreement was found, the derived fuselage normal areas were used in the wave drag program to obtain a revised set of equivalent areas due to volume. Combining these volume-induced equivalent areas with the existing lift-induced equivalent areas produced a total area distribution from which the pressure signature in figure 13 was calculated and compared with the ideal low-boom pressure signature. Again, a reasonably good agreement was found, indicating that the Mach 2 conceptual aircraft met the theoretical low-boom constraints at cruise. Although past conceptual supersonic cruise aircraft studies served as the basis for initiating the design, the integration of low sonic boom aircraft features changed the overall geometry sufficiently that it was necessary for a complete multidisciplinary vehicle and mission requirement study be done to determine how well each aspect of the specified mission was met.

Concluding Remarks

A systematic method for designing conceptual supersonic cruise aircraft to meet low sonic boom requirements has been outlined and described. Its use guides the aircraft design through a systematic evolution from initial wing planform and three-view drawing to a final numerical model description, and it permits the integration of low sonic boom, high supersonic aerodynamic efficiency, adequate low-speed handling, and reasonable structure and materials technologies. Some experience in preliminary aircraft design is required in the use of various analytical and numerical codes for integrating the volume and lift requirements throughout the design process.

NASA Langley Research Center
Hampton, VA 23665-5225
January 3, 1991

References

1. Whitham, G. B.: The Flow Pattern of a Supersonic Projectile. *Comm. Pure & Math.*, vol. V, no. 3, Aug. 1952, pp. 301–348.
2. Walkden, F.: The Shock Pattern of a Wing-Body Combination, Far From the Flight Path. *Aeronaut. Q.*, vol. IX, pt. 2, May 1958, pp. 164–194.
3. Jones, L. B.: Lower Bounds for Sonic Bangs. *J. Royal Aeronaut. Soc.*, vol. 65, no. 606, June 1961, pp. 433–436.
4. McLean, F. Edward: *Some Nonasymptotic Effects on the Sonic Boom of Large Airplanes.* NASA TN D-2877, 1965.
5. Carlson, Harry W.; McLean, F. Edward; and Shrout, Barrett L.: *A Wind-Tunnel Study of Sonic-Boom Characteristics for Basic and Modified Models of a Supersonic Transport Configuration.* NASA TM X-1236, 1966.
6. Seebass, R.; and George, A. R.: Sonic-Boom Minimization. *J. Acoust. Soc. America*, vol. 51, no. 2, pt. 3, Feb. 1972, pp. 686–694.
7. Middleton, Wilbur D.; and Carlson, Harry W.: *A Numerical Method for Calculating Near-Field Sonic-Boom Pressure Signatures.* NASA TN D-3082, 1965.
8. Carlson, Harry W.; Barger, Raymond L.; and Mack, Robert J.: *Application of Sonic-Boom Minimization Concepts in Supersonic Transport Design.* NASA TN D-7218, 1973.
9. Kane, Edward J.: *A Study To Determine the Feasibility of a Low Sonic Boom Supersonic Transport.* NASA CR-2332, 1973.
10. Darden, Christine M.: *Sonic-Boom Minimization With Nose-Bluntness Relaxation.* NASA TP-1348, 1979.
11. Mack, Robert J.; and Darden, Christine M.: *Wind-Tunnel Investigation of the Validity of a Sonic-Boom-Minimization Concept.* NASA TP-1421, 1979.
12. Harris, Roy V., Jr.: *A Numerical Technique for Analysis of Wave Drag at Lifting Conditions.* NASA TN D-3586, 1966.
13. Carlson, Harry W.; and Mack, Robert J.: *Estimation of Wing Nonlinear Aerodynamic Characteristics at Supersonic Speeds.* NASA TP-1718, 1980.
14. Mack, Robert J.: *A Numerical Method for Evaluation and Utilization of Supersonic Nacelle-Wing Interference.* NASA TN D-5057, 1969.
15. Carlson, Harry W.; and Miller, David S.: *Numerical Methods for the Design and Analysis of Wings at Supersonic Speeds.* NASA TN D-7713, 1974.
16. Hayes, Wallace D.; Haefeli, Rudolph C.; and Kulsrud, H. E.: *Sonic Boom Propagation in a Stratified Atmosphere, With Computer Program.* NASA CR-1299, 1969.
17. Mack, Robert J.; and Needleman, Kathy J.: *A Semiempirical Method for Obtaining Fuselage Normal Areas From Fuselage Mach Sliced Areas.* NASA TM-4228, 1990.

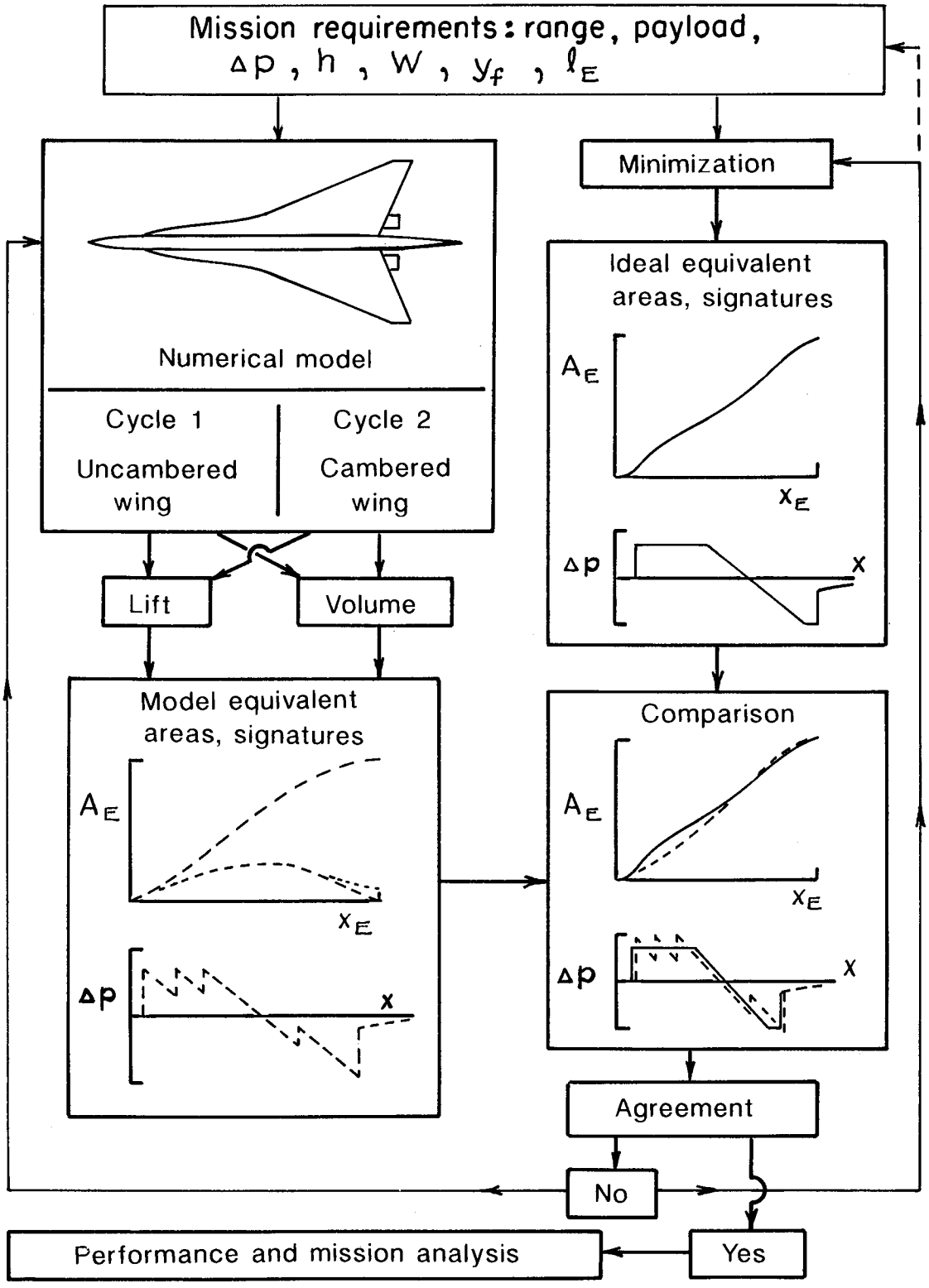

(a) Overall schematic.

Figure 1. Diagram of method.

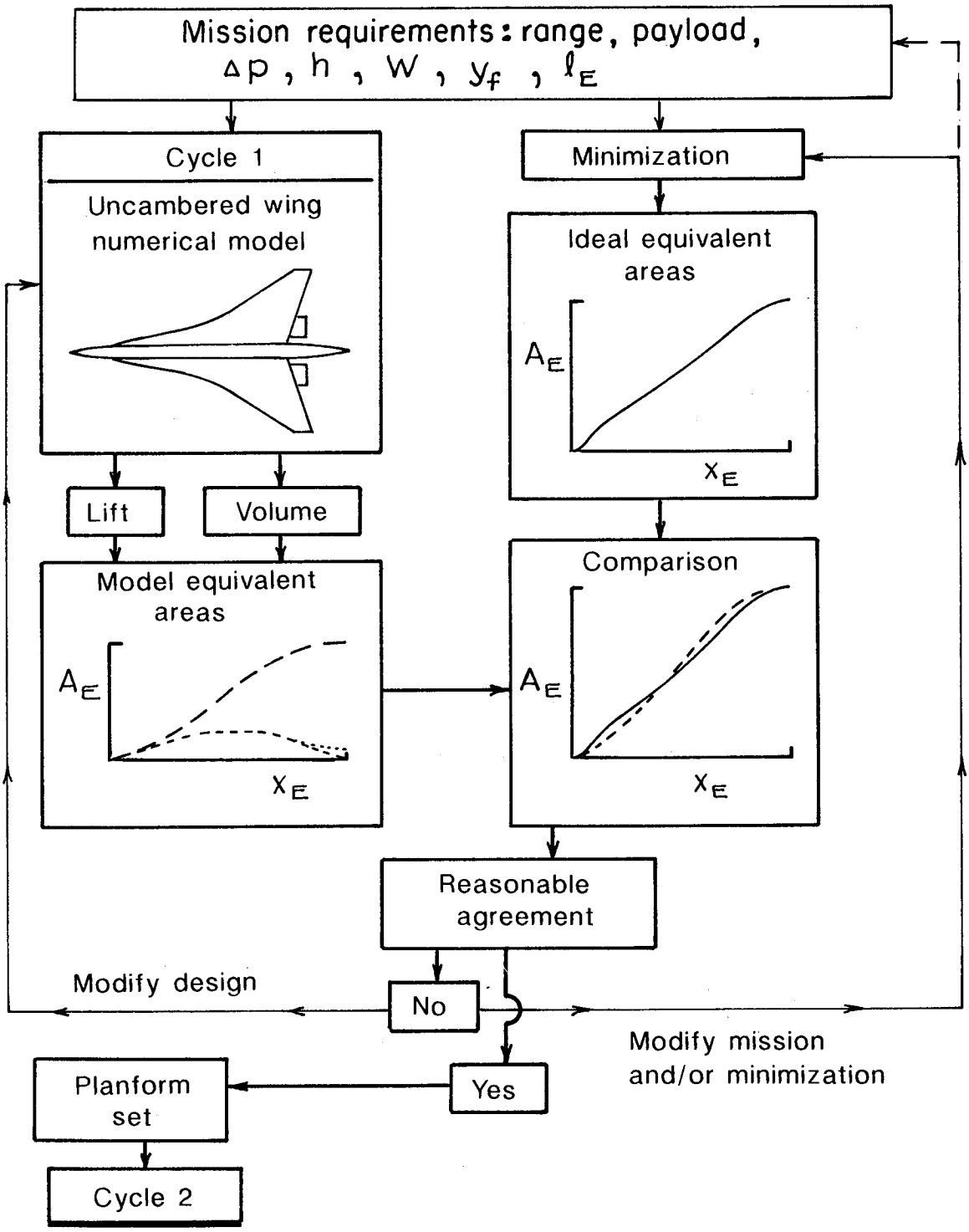

(b) Cycle 1: determination of the aircraft planform and the initial three-view.

Figure 1. Continued.

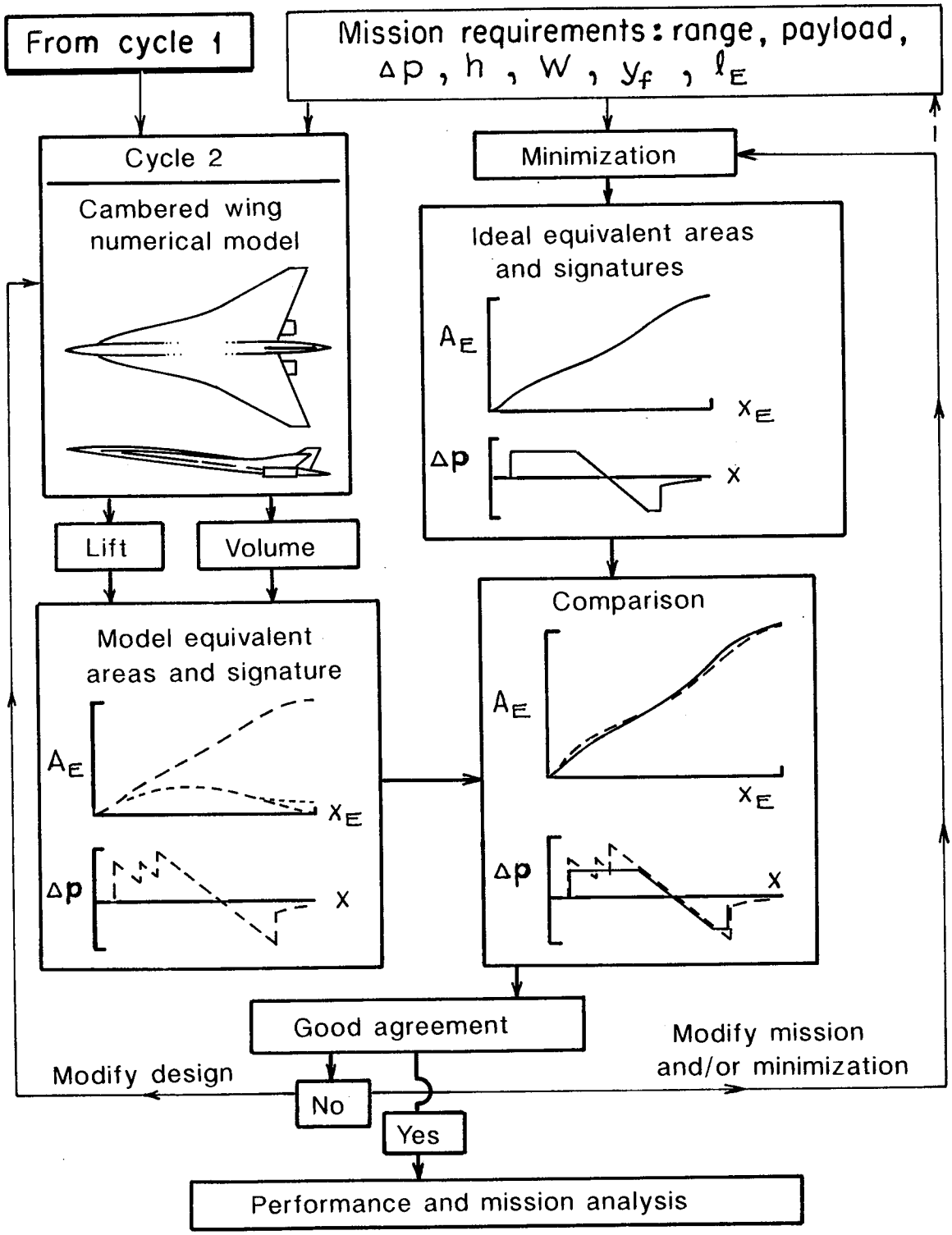

(c) Cycle 2: determination of the camber surface and low-boom aircraft geometry.

Figure 1. Concluded.

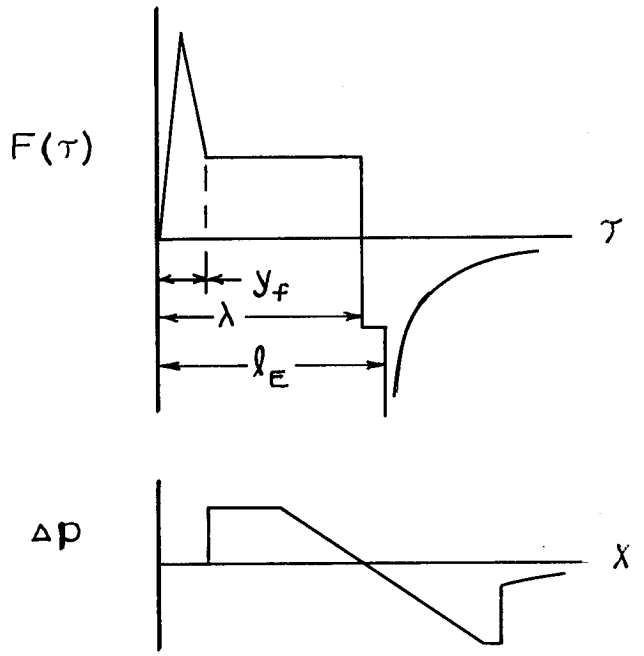

(a) Minimum overpressure F-function and signature.

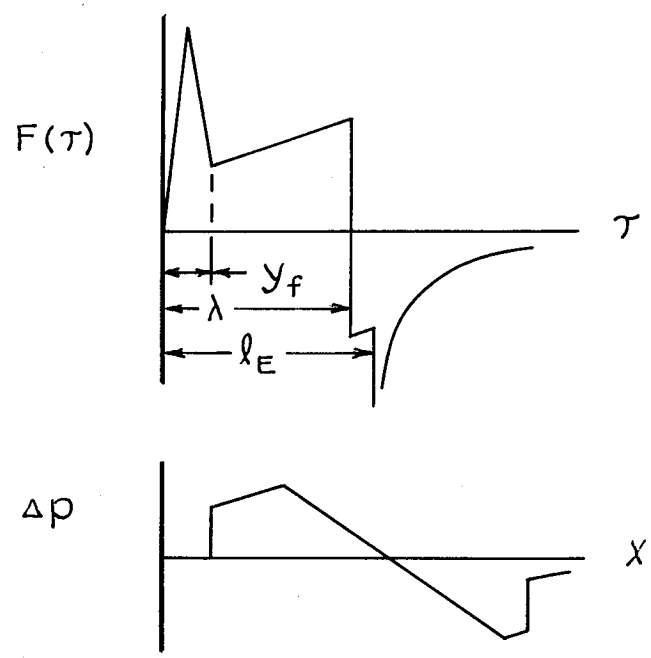

(b) Minimum nose-shock F-function and signature.

Figure 2. F-functions and pressure signatures from minimization code (ref. 8).

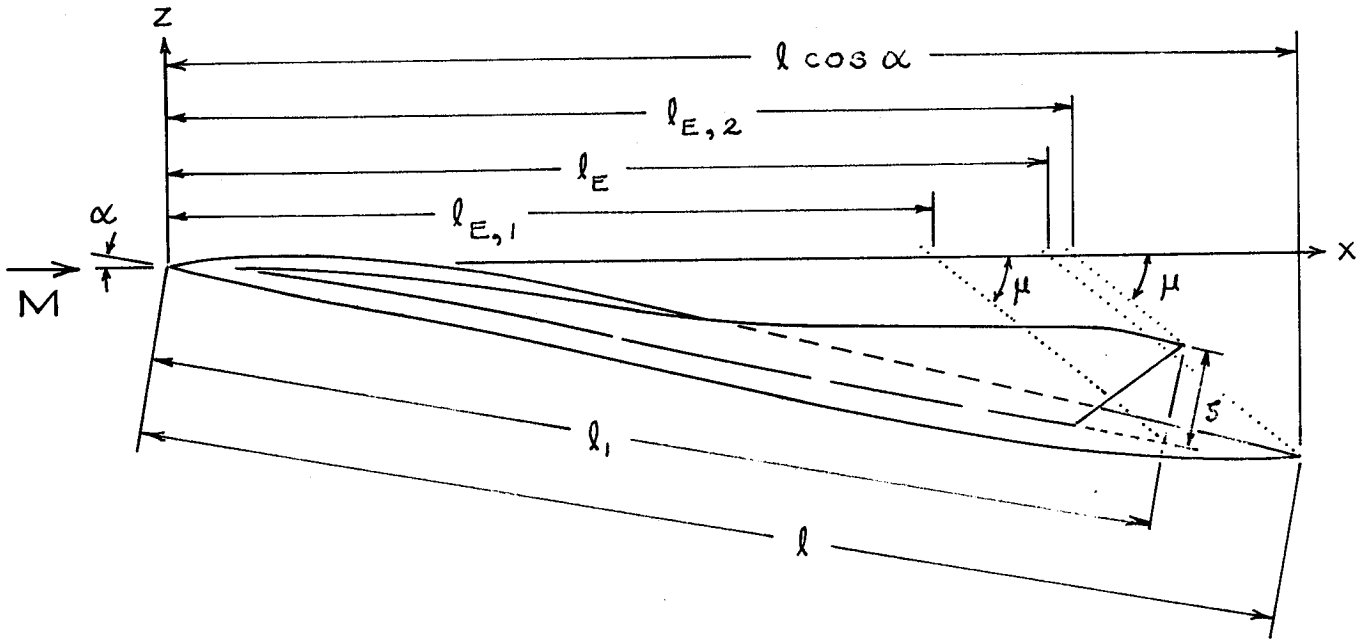

Figure 3. Effect of angle of attack and dihedral on effective length.

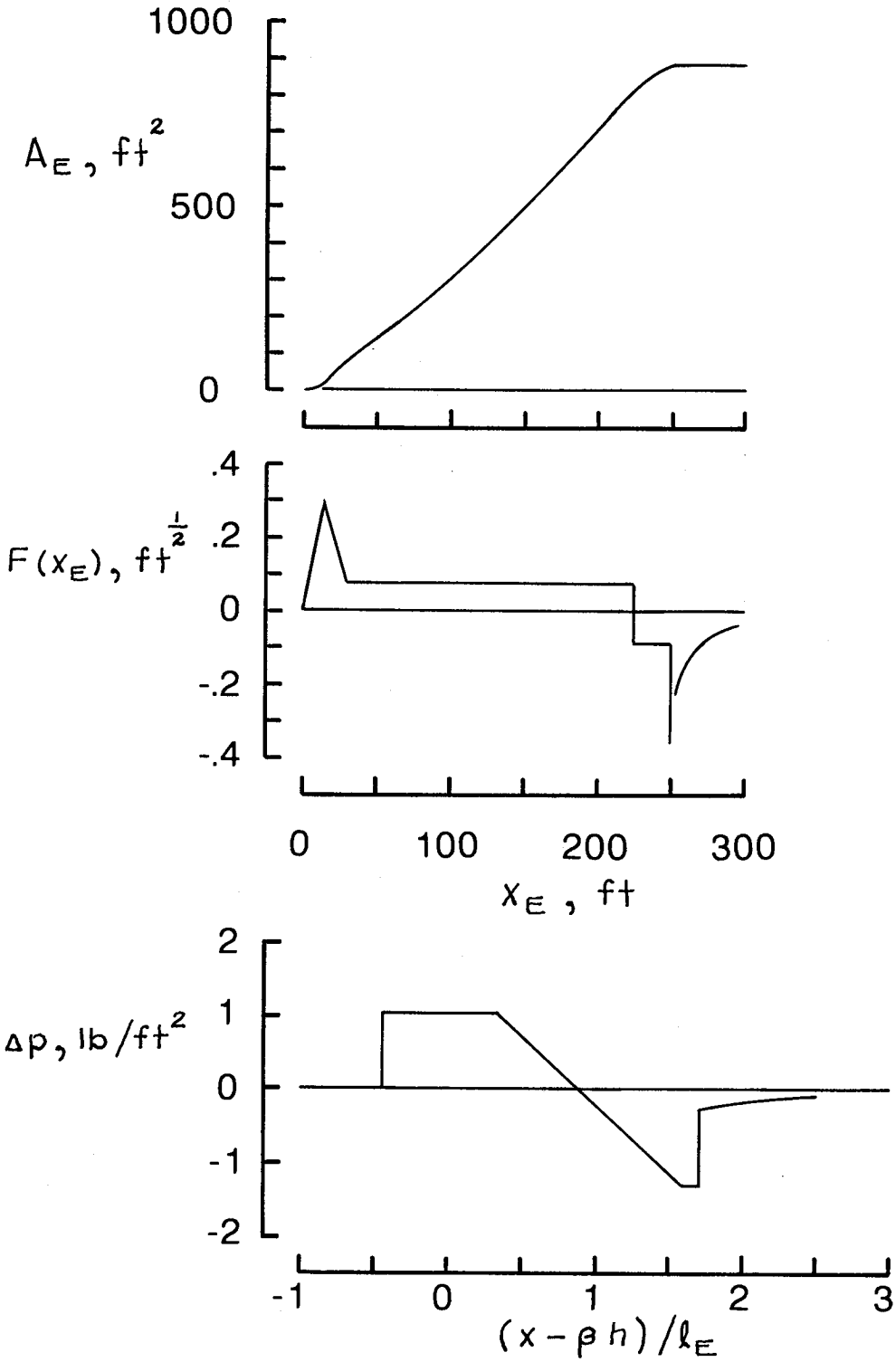

Figure 4. Initial equivalent-area distribution, Whitham F-function, and pressure signature for a Mach 2.0 low-boom concept.

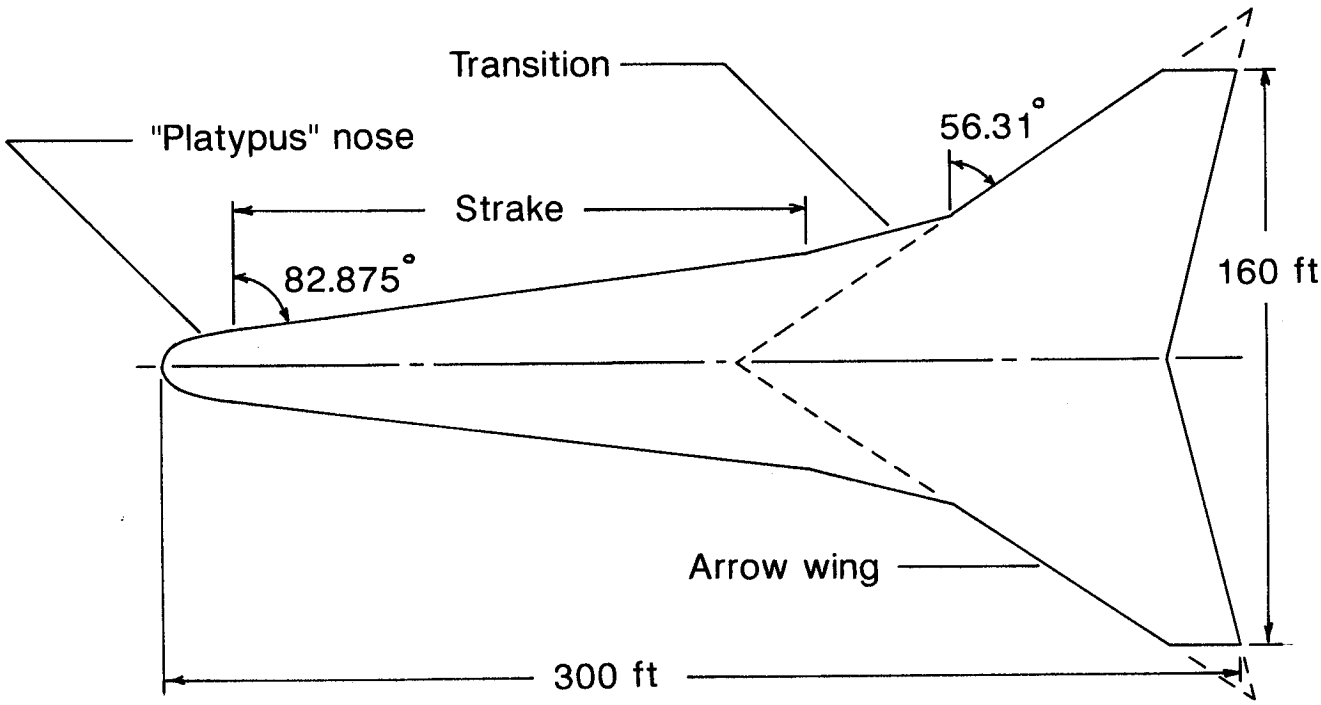

Figure 5. Initial wing planform.

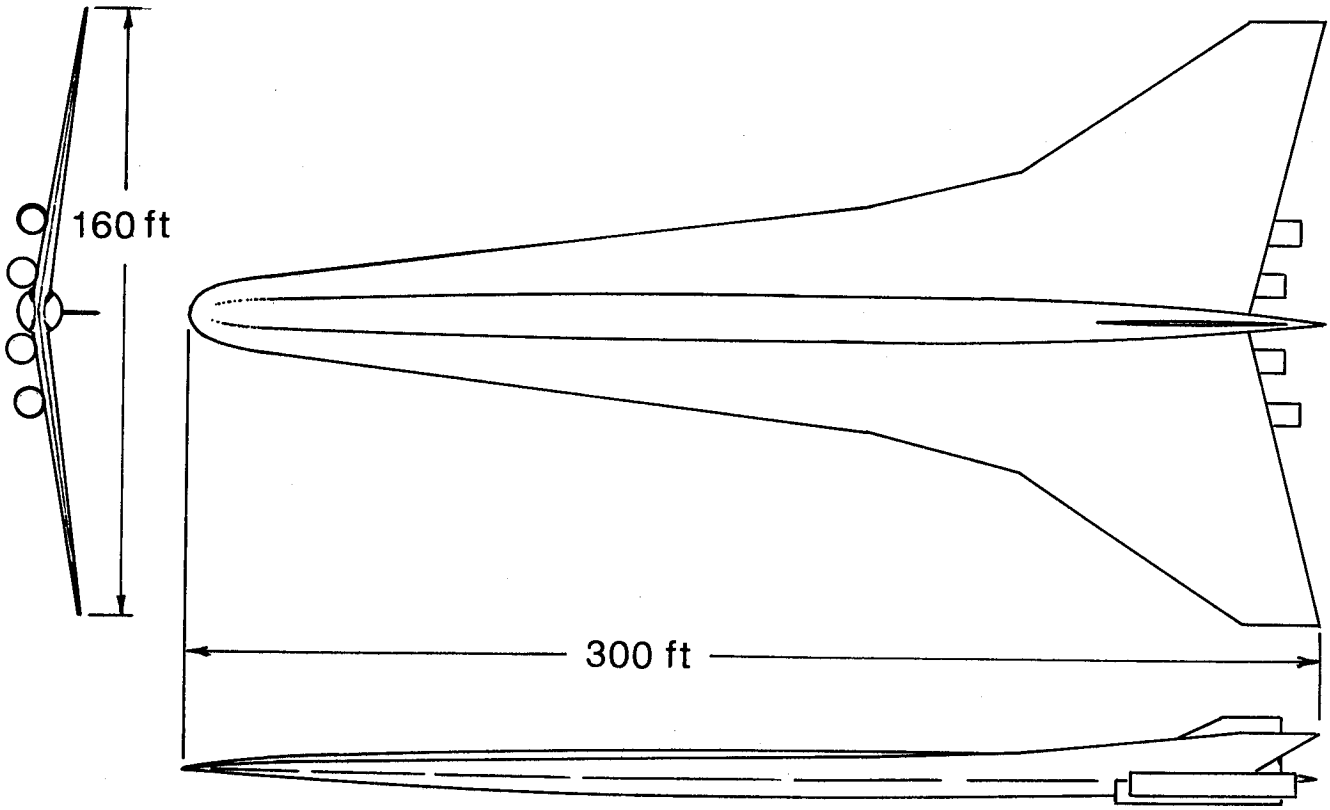

Figure 6. Three-view of initial Mach 2.0 conceptual aircraft.

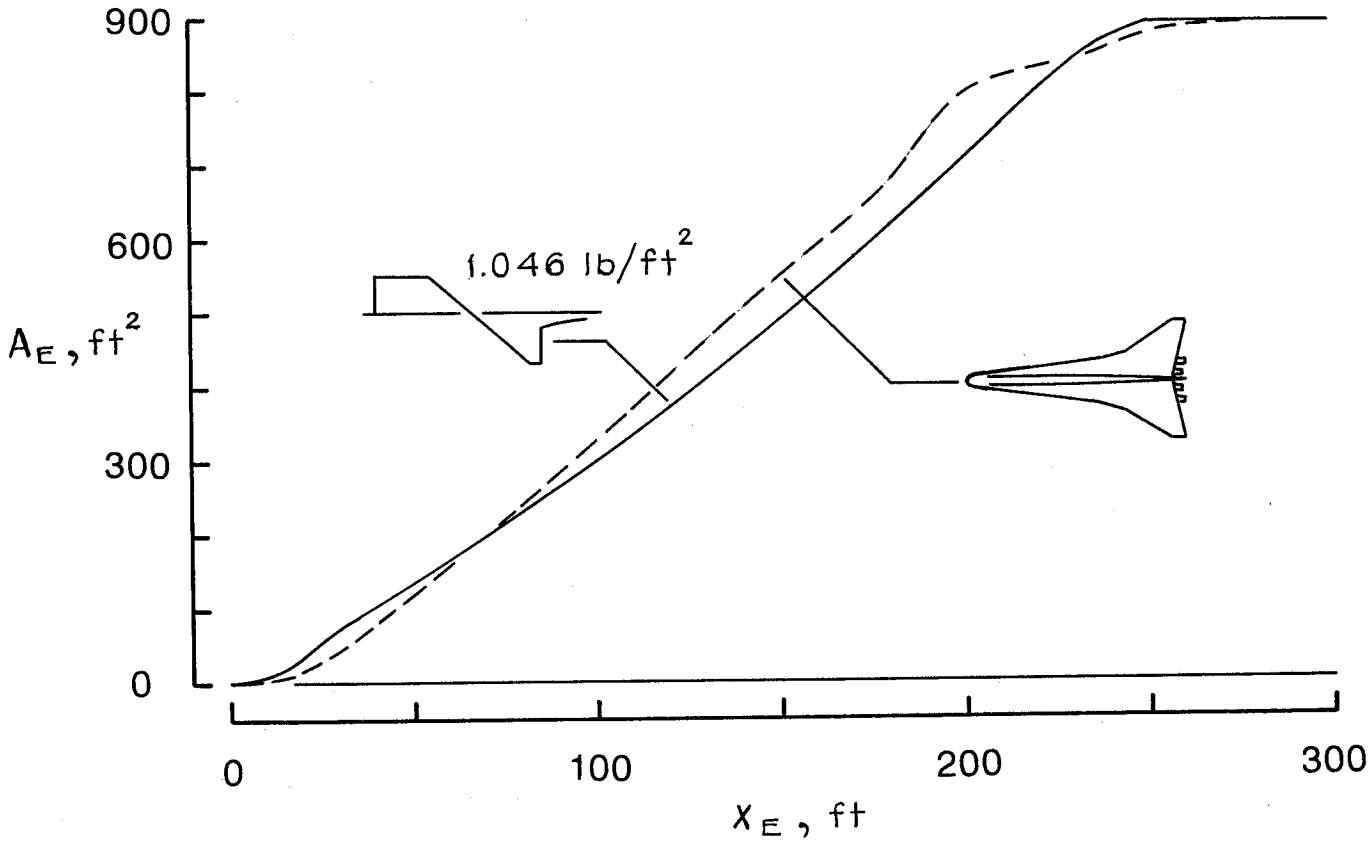

Figure 7. Comparison of equivalent areas from the initial Mach 2.0 concept and the low-boom constraint curve.

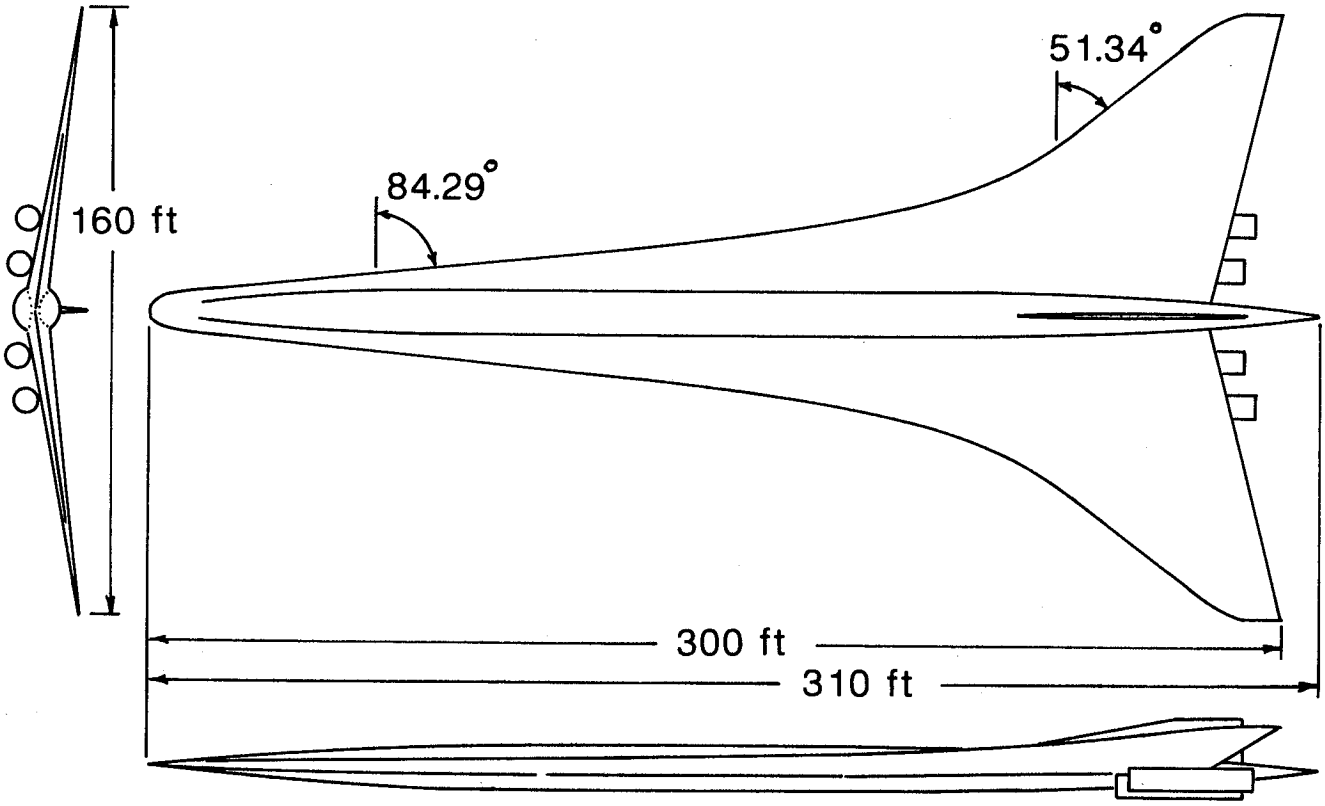

Figure 8. Three-view of modified Mach 2.0 conceptual aircraft with flat-plate camber surface.

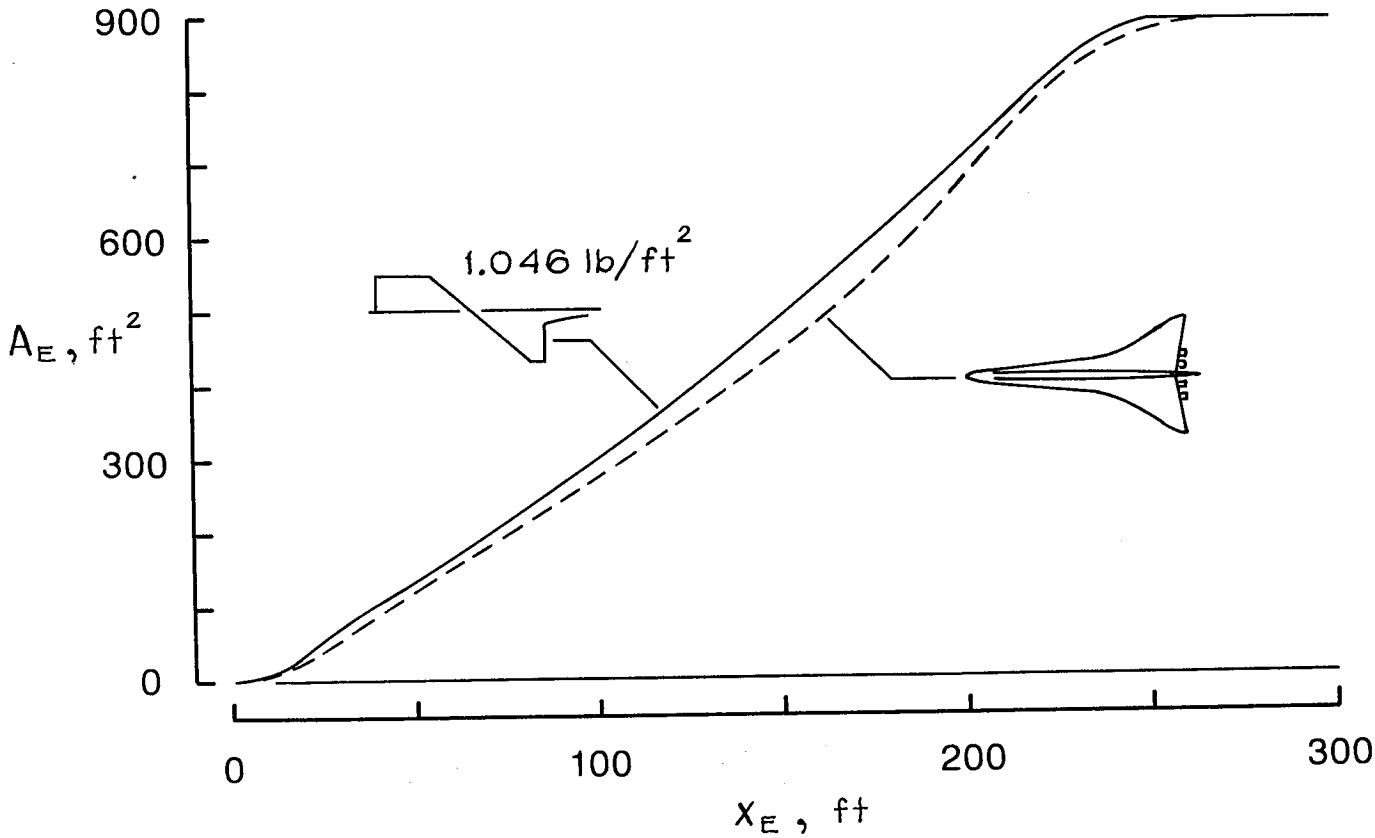

Figure 9. Comparisons of equivalent areas from the modified Mach 2.0 conceptual aircraft and the low-boom constraint curve.

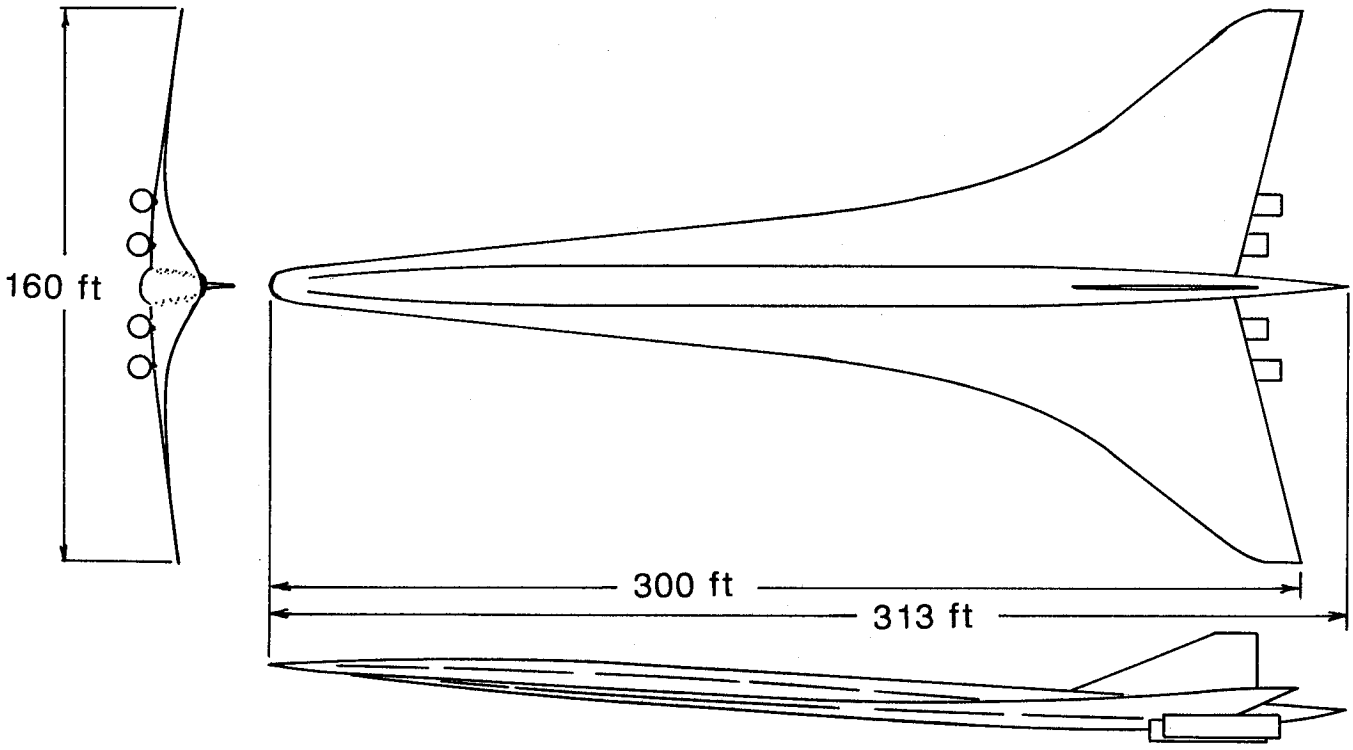

Figure 10. Three-view of the Mach 2.0 conceptual aircraft with cambered and twisted wing surface.

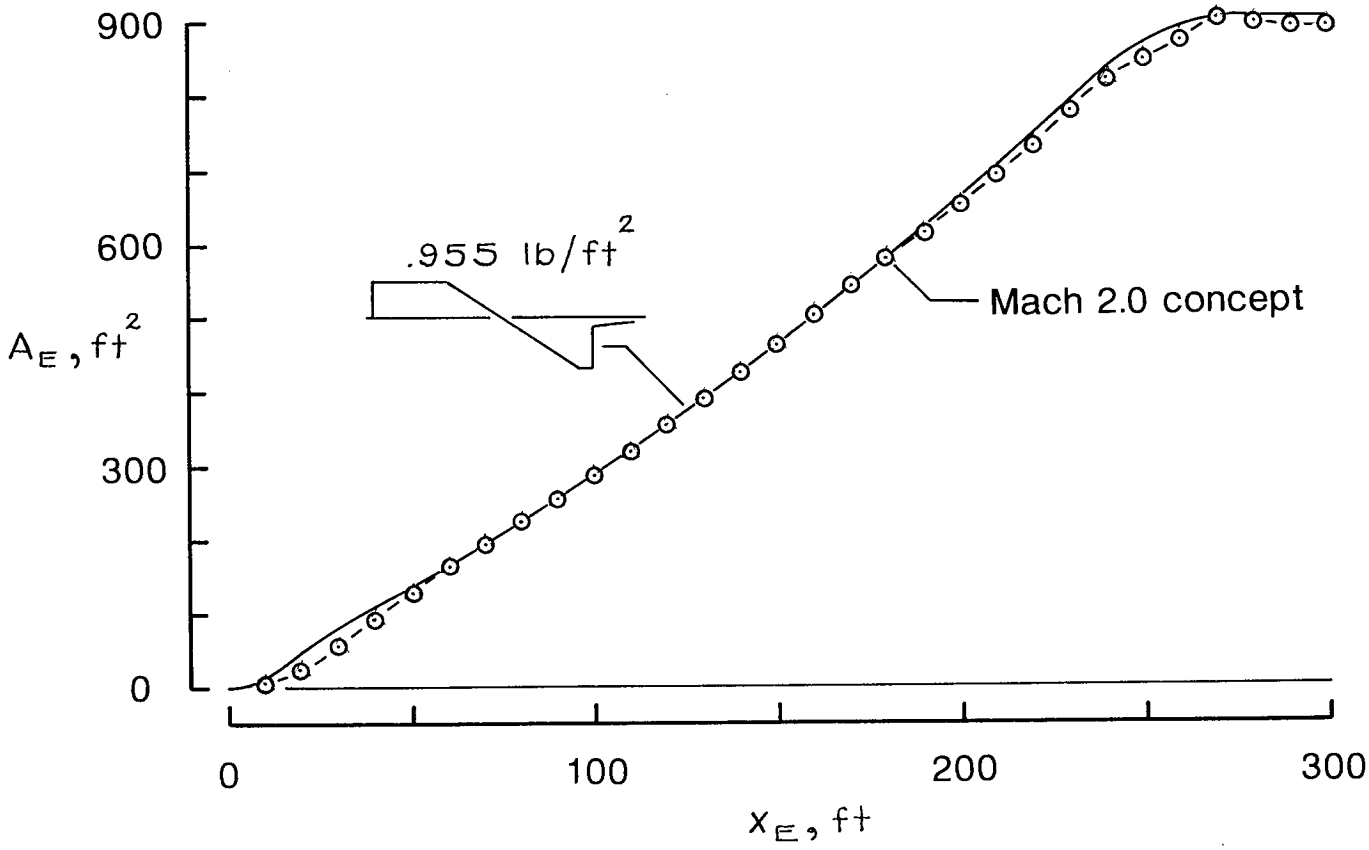

Figure 11. Comparison of equivalent areas from the recalculated low-boom constraint curve and the modified Mach 2.0 conceptual aircraft with cambered and twisted wing.

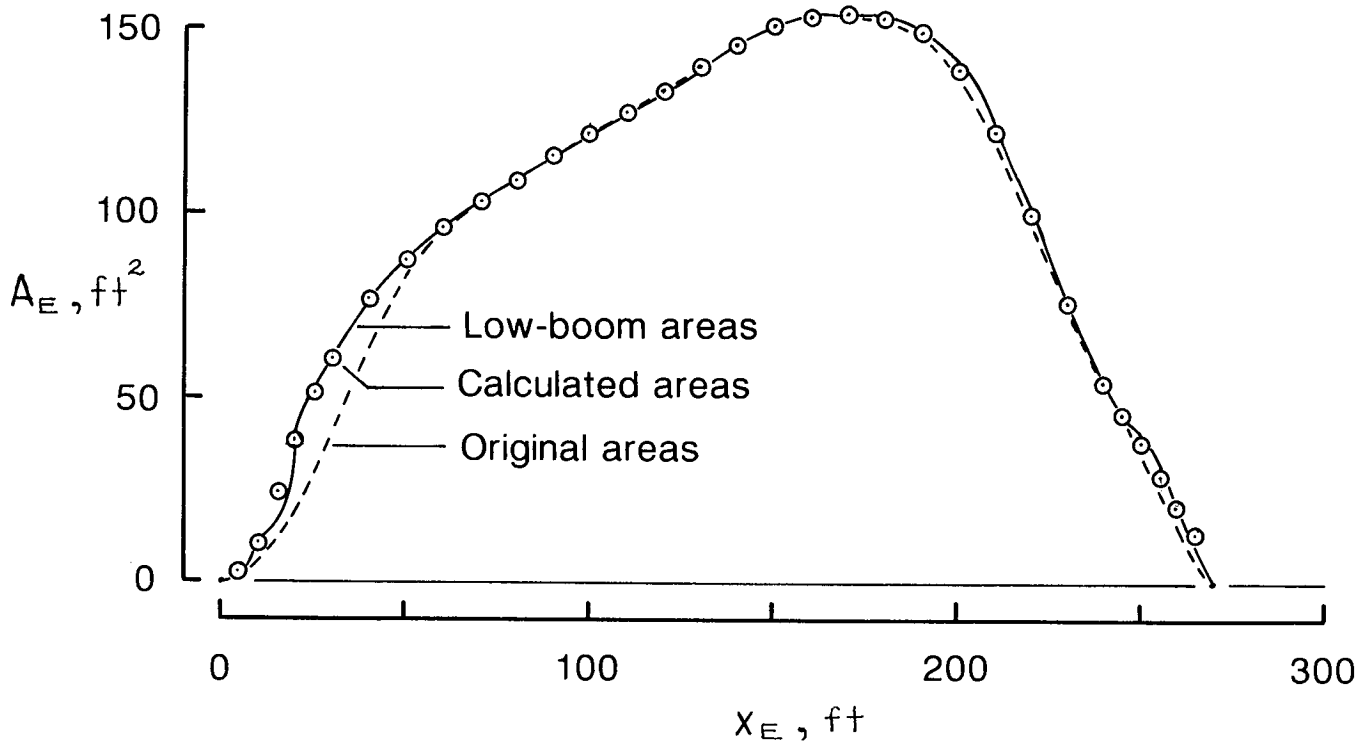

Figure 12. Comparison of fuselage equivalent areas from low-boom constraint curve with areas calculated from method of reference 15.

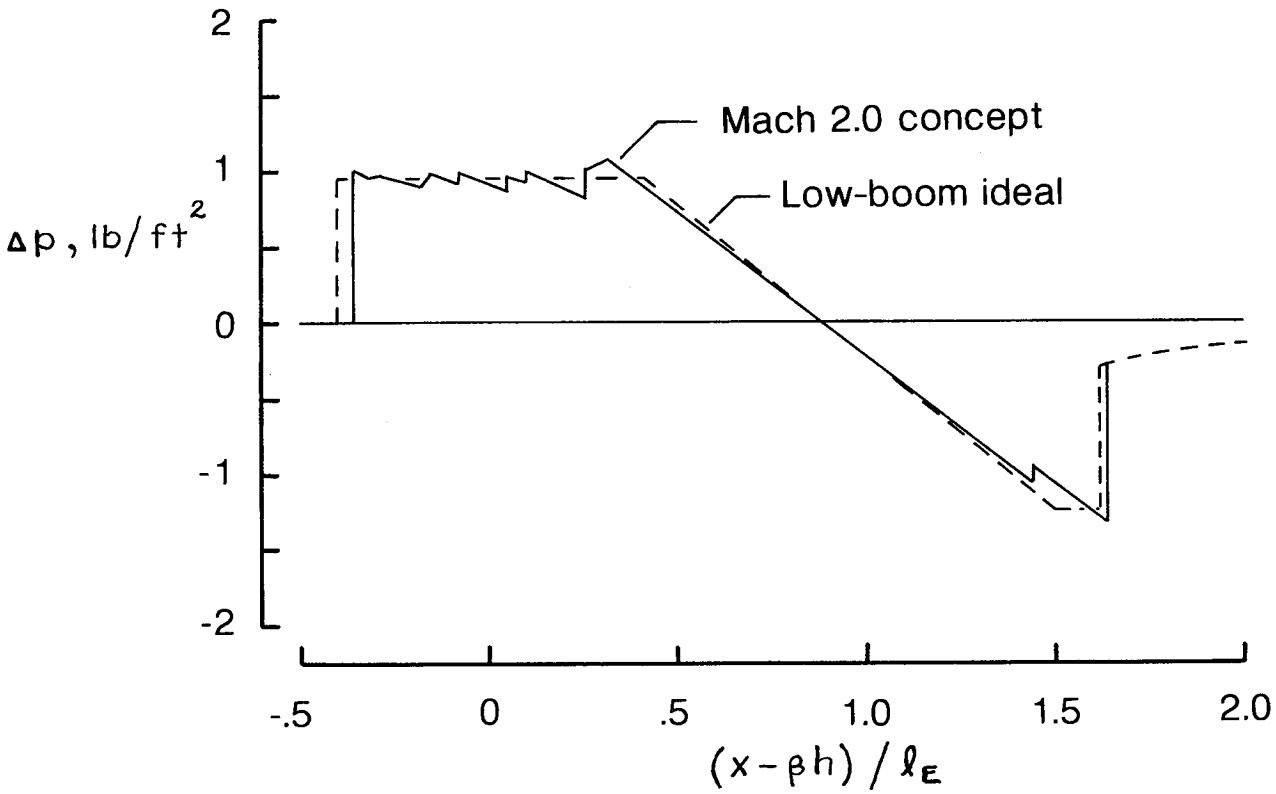

Figure 13. Comparison of the ideal low-boom signature with the Mach 2.0 conceptual aircraft signature.

NASA
National Aeronautics and Space Administration

Report Documentation Page

1. Report No.	2. Government Accession No.	3. Recipient's Catalog No.
NASA TM-4246		

4. Title and Subtitle	5. Report Date
A Methodology for Designing Aircraft to Low Sonic Boom Constraints	February 1991
	6. Performing Organization Code
7. Author(s)	8. Performing Organization Report No.
Robert J. Mack and Kathy E. Needleman	L-16768
9. Performing Organization Name and Address	10. Work Unit No.
NASA Langley Research Center Hampton, VA 23665-5225	537-03-21-01
	11. Contract or Grant No.
12. Sponsoring Agency Name and Address	13. Type of Report and Period Covered
National Aeronautics and Space Administration Washington, DC 20546-0001	Technical Memorandum
	14. Sponsoring Agency Code

15. Supplementary Notes

Robert J. Mack: Langley Research Center, Hampton, Virginia.
Kathy E. Needleman: Lockheed Engineering & Sciences Company, Hampton, Virginia.

16. Abstract

A method for designing conceptual supersonic cruise aircraft to meet low sonic boom requirements has been outlined and described. The aircraft design is guided through a systematic evolution from an initial three-view drawing to a final numerical model description while the designer using the method controls the integration of low sonic boom, high supersonic aerodynamic efficiency, adequate low-speed handling, and reasonable structure and materials technologies. Some experience in preliminary aircraft design and in the use of various analytical and numerical codes is required for integrating the volume and lift requirements throughout the design process.

17. Key Words (Suggested by Authors(s))	18. Distribution Statement
Sonic boom Aircraft design Low-boom methodology	Unclassified—Unlimited Subject Category 05

19. Security Classif. (of this report)	20. Security Classif. (of this page)	21. No. of Pages	22. Price
Unclassified	Unclassified	22	A03

NASA FORM 1626 OCT 86

NASA-Langley, 1991

For sale by the National Technical Information Service, Springfield, Virginia 22161-2171